EARTH SURFACE PROCESSES AND LANDFORMS
Earth Surf. Process. Landforms **36**, 1209–1217 (2011)

Published online 21 March 2011 in Wiley Online Library
(wileyonlinelibrary.com) DOI: 10.1002/esp.2146

Dendrogeomorphic dating of rockfalls on low-latitude, high-elevation slopes: Rodadero, Iztaccíhuatl volcano, Mexico

Markus Stoffel,[1,2]* Michelle Bollschweiler,[1,2] Lorenzo Vázquez-Selem,[3] Osvaldo Franco-Ramos[3] and David Palacios[4]
[1] Laboratory of Dendrogeomorphology, Institute of Geological Sciences, University of Berne, Berne, Switzerland
[2] Department for Environmental Sciences, University of Geneva, Carouge, Switzerland
[3] Instituto de Geografía, Universidad Nacional Autónoma de México (UNAM), México D.F., Mexico
[4] Department of Physical Geography, Complutense University, Madrid, Spain

Received 17 March 2010; Revised 7 February 2011; Accepted 8 February 2011

* Correspondence to: M. Stoffel, Laboratory of Dendrogeomorphology, Institute of Geological Sciences, University of Berne, Baltzerstrasse 1+3, CH-3012 Berne, Switzerland. E-mail: markus.stoffel@dendrolab.ch

ESPL
Earth Surface Processes and Landforms

ABSTRACT: Dynamics and rates of rockfalls have been repeatedly studied in mountain environments with archival records as well as lichenometric, radiocarbon or dendrogeomorphic approaches. In this study, we test the potential of conifers growing at a low-latitude, high-elevation site as a dendrogeomorphic tool to reconstruct to calendar dates associated rockfall activity. Analysis is based on tree-ring records of Mexican mountain pine (*Pinus hartwegii* Lindl.) growing at timberline [~4000 m above sea level (a.s.l.)] and at the runout fringe of a north–northeast (NNE)-facing slope of the dormant Iztaccíhuatl volcano (Mexico), which is subject to frequent rockfalls. The potential and limitations of tree-ring data are demonstrated based on 67 rockfall impacts dated in the increment-ring series of 24 trees since AD 1836. While findings of this paper are site-specific, the study clearly shows the potential of dendrogeomorphic approaches in extra-Alpine, low-latitude environments and for the understanding of rockfall processes in space and time. Copyright © 2011 John Wiley & Sons, Ltd.

KEYWORDS: rockfall; injury; tree ring; dendrogeomorphology; talus slope; volcano; Mexico; *Pinus hartwegii* Lindl

Introduction

Rockfalls are one of the most intensely studied geomorphic processes in steep Alpine and peri-glacial environments (Luckman and Fiske, 1995) with an overwhelming concentration of damage in talus foot settlements, particularly in developing countries of the lower latitudes (Hewitt, 1976). Rockfalls are defined here as the free or bounding fall of rock debris down steep slopes varying in volume from individual small pebbles to catastrophic failures of several million cubic meters (Luckman, 2007). Rock fragments can be detached from bedrock along pre-existing or new discontinuities or can be dislodged from irregularities in the cliff after temporal accumulation (Dorren, 2003). Triggering mechanisms of rockfalls include earthquakes (Harp and Wilson, 1995; Marzorati *et al*., 2002; Becker and Davenport, 2003), freeze–thaw cycles of interstitial water (Matsuoka and Sakai, 1999; Matsuoka and Murton, 2008), thawing of permafrost (Gruber *et al*., 2004) or intense rainfall (Cardinali *et al*., 2006). Several inventory studies have, in addition, identified diurnal maxima of rockfalls during times of solar illumination or precipitation and seasonal maxima in spring and fall (Rapp, 1960; Luckman, 1976).

Below the preferential failure surface, pebbles, rocks and boulders will be deposited as soon as they have lost enough energy in impacts or friction (Guzzetti and Reichenbach, 2010) and as a result of decreasing slope steepness. The accumulation of discrete rockfalls over long periods of time will result in the formation of talus slopes or talus cones (Luckman, 2007). If talus slopes or the runout fringe of boulders beyond the talus foot are covered with forests, individual rockfall fragments may damage or even destroy trees along their trajectory (Stoffel, 2006). Woody vegetation damaged by rockfalls or growing on talus provides a valuable means for dating and interpreting past rockfalls with high accuracy and over long periods of the past (Stoffel *et al*., 2010). Dendrogeomorphic methods (Alestalo, 1971; Shroder, 1978) aim at inferring data on past processes from information preserved in tree rings. Previous tree-ring research primarily focused on the reconstruction of rockfall frequencies (Stoffel *et al*., 2005b; Perret *et al*., 2006; Schneuwly and Stoffel, 2008a), the extent and magnitude of rockfalls (Stoffel *et al*., 2005b), the triggering of rockfalls resulting from heavy rainfall or seismic events (Schneuwly and Stoffel, 2008b), its seasonality (Stoffel *et al*., 2005a) or on the comparison of observed rockfall data with activity predicted by three-dimensional, process-based models (Stoffel *et al*., 2006). More recently, rockfall research has included broad-leaved trees growing on talus slopes to document recent activity (Moya *et al*., 2010).

Despite the destructive potential of rockfalls and the considerable number of casualities, rockfall–tree-ring research remains in its infancy and only a very limited number of talus slopes has been analyzed with dendrogeomorphic approaches to date. Trees growing outside the mountain ranges of mid- or high-latitude environments have been used occasionally for dendroclimatic or dendroecologic research, but did not form the subject of mass-movement analyses in the past.

It is therefore our goal of this study to test the potential of dendrogeomorphic approaches within a low-latitude, high-elevation context where the assessment of natural hazards is often hampered by rather limited databases on past events. Possibilities and limitations of reconstructing spatio-temporal patterns of and changes in rockfall activity are shown for a site at the base of Rodadero talus cone of Iztaccíhuatl volcano (Mexico). Analyses were performed with Mexican mountain pine (*Pinus hartwegii* Lindl.), a species which has rarely been used in dendrogeomorphic research so far and which forms the upper forest belt above 3600 m above sea level (a.s.l.) on the mountains of central Mexico (Beaman, 1962; Lauer, 1978). We report 67 rockfalls observed in the tree-ring series of 24 trees (86 samples) since AD 1836, demonstrate the benefits of tree-ring records at high-elevation, low-latitude sites and illustrate how diameter growth of trees and sample depth may influence impact probabilities and thus bias reconstructed rockfall frequencies.

Study Site

The site investigated in this study is called Rodadero and is located on the north-northeast (NNE)-facing slopes of Iztaccíhuatl, a volcano that was built throughout the Pleistocene (Nixon, 1989). Iztaccíhuatl had its latest dated activity around the Pleistocene-Holocene transition (Siebe *et al.*, 1996), and is nowadays considered dormant. In addition, late Pleistocene and Holocene glaciations have been documented on Iztaccíhuatl (White, 1962; Vázquez-Selem, 1997; Vázquez-Selem and Heine, 2004).

On the NNE-facing slope of Téyotl peak (the northernmost component of Iztaccíhuatl), frequent rockfalls out of a Quaternary glacier cirque has formed an impressive talus cone extending from 4320 m to 3980 m a.s.l. (17 ha; 19° 13′ 7′′ N, 98° 38′ 6′′ W; Figures 1 and 2A). Toponomy (*rodadero* = a place where elements row downhill) alludes to the presence of frequent rockfalls at the study site. In addition, satellite images and local morphology point to the sporadic occurrence of small snow slides and associated boulder tongues in the upper part of the slope and in the vicinity of the cliffs above the study site. Poorly developed channel heads and a limited number of associated levees and lobate deposits are observed in the west-northwest (WNW) part of the cirque, alluding to the existence of (infrequent) debris flows. At the site selected for analysis, however, talus slope is characterized by rocky unchanneled topography and signs of mass-wasting processes other than rockfalls or isolated reworking of sediment by small hillslope debris flows are clearly missing. Glaciers are absent in the cirques under current climatic conditions and signs of contemporary permafrost are clearly missing on the talus slope above the study site, but very localized, centimetric ice layers have been observed at the base of the rockfall talus WNW of the study site.

Meteorological data from stations located near Iztaccíhuatl indicate that >85% of annual precipitation falls from May to October, mostly in the form of rain pours or hail events, and that <5% of annual precipitation occurs in winter (i.e. January–March). Data from a station located at 4140 m on Nevado de Toluca (the only high-elevation weather station in central Mexico) shows that mean annual precipitation oscillates around 1250 mm. Precipitation totals >20 mm d^{-1} are common, and values >70 mm d^{-1}, although very rare, have been recorded as well. Winter precipitation is in the form of snowfall associated

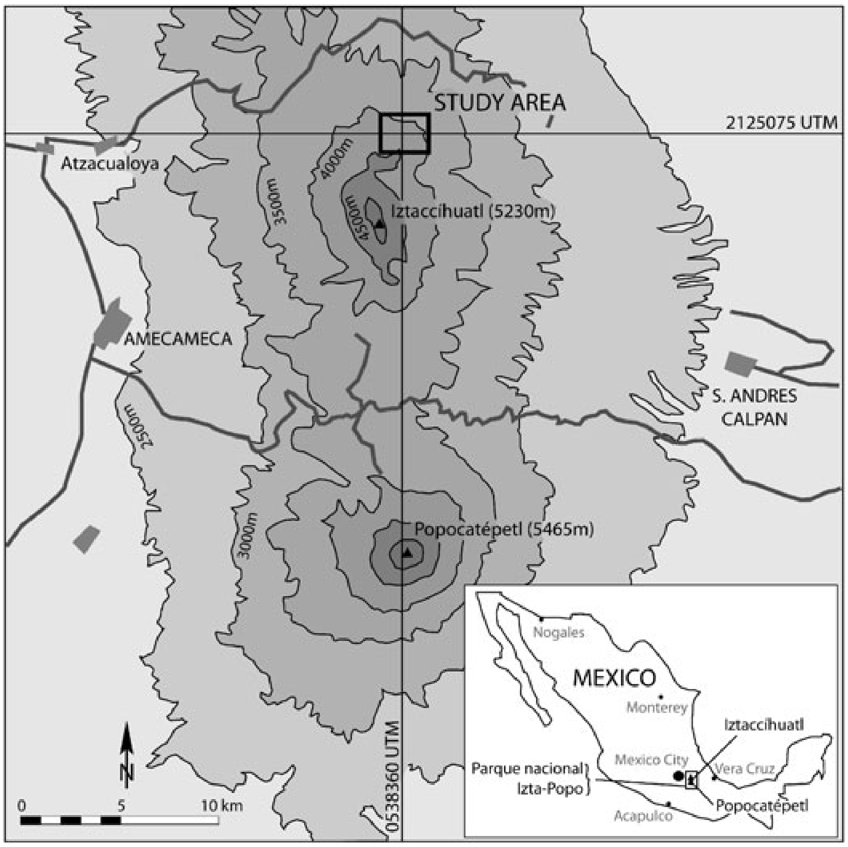

Figure 1. The Rodadero talus slope is located on the NNE-facing slope of Iztaccíhuatl volcano (Téyotl peak), Trans-Mexican volcanic belt.

with episodic cold fronts, but the resulting snow cover (in general <0·2 m at Rodadero) lasts only for a few days.

At the study site, the volume of single rockfall fragments does not normally exceed 0·5–1 m^3, but few blocks deposited beyond the talus foot with volumes of up to ~5 m^3 bear witness to major events in the past. Bedrock in the release area consists of densely jointed dacite belonging to the Téyotl unit (~80 ka) as mapped by Nixon (1989). Of relatively young age and exposed to cool climate with sparse grass vegetation (i.e. bunch grass and *Juniperus monticola*), the locally brecciated bedrock is widely jointed (spacing >20 cm) and only faintly weathered. Rockfall fragments are usually released from the (sub-)vertical cliffs of the cirque and travel down the ~35° talus slope. The size distribution of rockfall fragments on the talus slope points to an early deposition of smaller rocks in its upper part and larger travel distances for boulders. Differences in the state of weathering and in joint denisty have resulted in preferential release areas, preferential trajectories and the formation of several cone-shaped talus bodies at the study site. A decimetric soil layer covers the lowermost parts of the talus, whereas the surfaces higher up on the cone remain free of vegetation (Figures 2B and 3). Individual *Pinus hartwegii* trees colonize the base of the talus cone, but a continuous timberline with adult trees is only present at the runout fringe of rocks and boulders beyond the talus foot at 3950 m a.s.l., corresponding more or less to natural local timberline which locally oscillates at 4020 ± 50 m a.s.l. (Beaman, 1962).

The forest chosen for analysis grows at the contact of the talus slope with the talus foot; it is 120 m wide, 35 m large and covers a surface of ~3000 m^2. Mean slope angles at the study site average 28° with only minor variations between its top and bottom. Signs of anthropogenic activity (i.e. farming, extraction of firewood and construction wood) are missing in the forest,

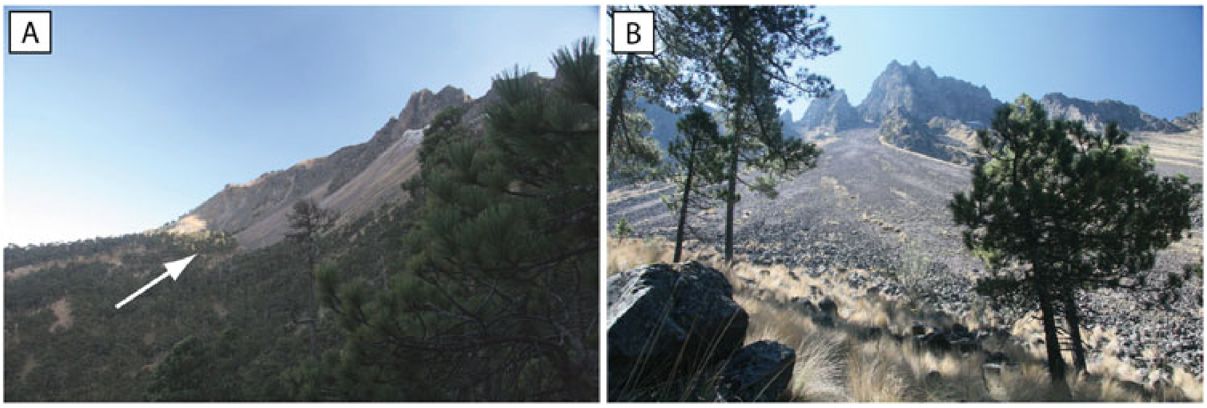

Figure 2. (A) Overview of the study site with the release areas of rockfalls and the talus slopes. The arrow indicates the site chosen for analyses. (B) View upslope from the study site to the departure zone of rocks and boulders. This figure is available in colour online at wileyonlinelibrary.com/journal/espl

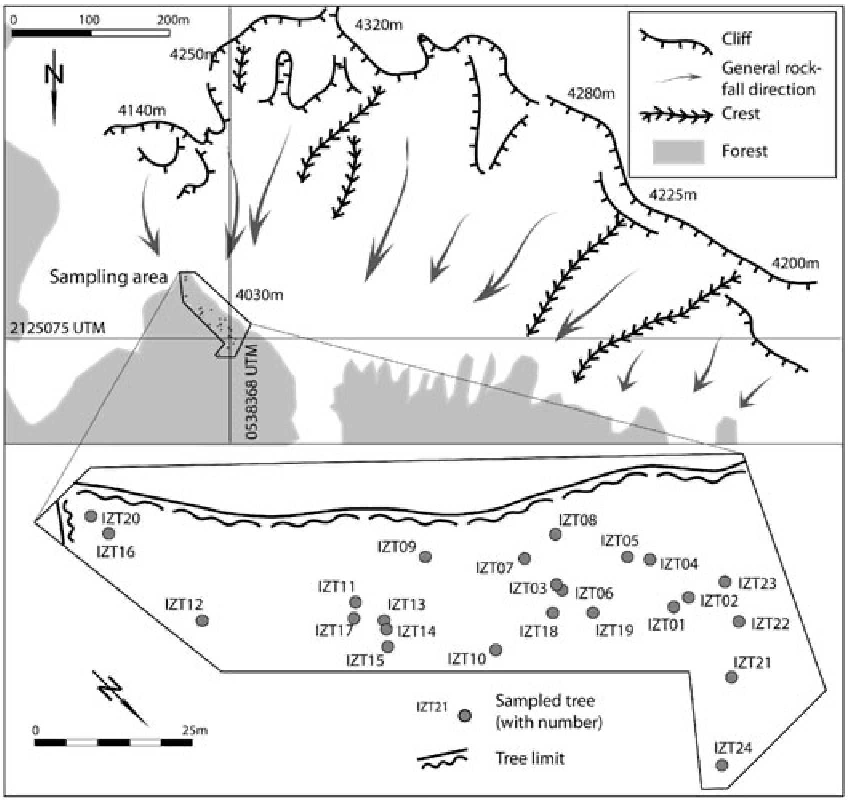

Figure 3. A total of 24 *Pinus hartwegii* Lindl. trees have been chosen for analysis at the study site. Most of the samples selected form the local timberline at *c.* 3950 m a.s.l.

either at the study site itself or in neighboring forested sectors. In contrast, there is evidence of past forest fires in a limited number of century-old *Pinus hartwegii* trees.

Material and Methods

Sampling strategy

At the study site, virtually all trees show externally visible growth anomalies in the stem resulting from past rockfalls in the form of injuries, broken crowns or branches, and tilted stems. As scars represent the most accurate and reliable growth disturbance (GD) to date past rockfalls in tree-ring records (Stoffel, 2005; Schneuwly and Stoffel, 2008b), we actively searched for visible stem wounds (Figure 4) and apex loss (i.e. tree topping). Trees to be sampled were selected so as to investigate the entire stand and to assure an even distribution of trees throughout the study site.

Sampling of trees was undertaken using two different methods: (i) on the one hand, we used a small handsaw to obtain cross-sections from each injury of trees with a basal diameter <10 cm; (ii) on the other hand, we extracted cores (maximum 40 cm × 5 mm) with increment borers. Injuries in bigger trees (<10 cm) were sampled with at least one core per scar, with cores extracted from the overgrowing tissue at the height showing the maximum wound extension (Schneuwly *et al.*, 2009a; Schneuwly *et al.*, 2009b). As the extraction of cores from the overgrowing callus needs to be effected at the contact of the injured with the non-injured tissue, normally more than one sample had to be taken to obtain adequate core samples (Stoffel and Bollschweiler, 2008). We also extracted an increment core from the downslope side of trees to (i) control dating on the upper side; and to (ii) determine abrupt growth decrease in topped and/or heavily injured trees. To avoid doubtful results, we did not sample trees with signs of fire-induced GD.

In addition, data recorded for each tree included micro-topography or the accumulation of rockfall deposits in the immediate vicinity of the tree. We also noted tree-specific data including tree height, its diameter at breast height (DBH), and comments on neighboring trees. In addition, all visible defects in its morphology (such as scar direction, surface and height of center above ground level, broken crowns or branches, and tilted stems or candelabra growth) were recorded and general pictures of the tree as well as one photograph per wound were taken to facilitate rockfall reconstruction in the laboratory. In a final step and in the case of increment cores, we noted the height and direction of each core sample. In total, 24 *Pinus hartwegii* trees were chosen and 86 samples taken (82 increment cores, four cross-sections). The spatial distribution of trees sampled is given in Figure 3.

Sample analysis and dating of events

In the laboratory, tree samples were analyzed and data processed following the standard procedures described by Bräker (2002). Single steps of sample analysis included surface preparation and ring-width measurements using digital LINTAB positioning tables connected to a Leica stereomicroscope and TSAP 4.63 (Time Series Analysis and Presentation) software (Rinntech, 2010). Growth curves of the disturbed samples were then cross-dated using the standard correlation parameters of TSAP 4.63 (Rinntech, 2010) to separate insect or climatically driven fluctuations in tree growth from abrupt GD (i.e. scars, callus tissue, compression wood, abrupt growth decrease or recovery; see Stoffel *et al.*, 2010, and references cited therein for details) caused by falling rocks (Cook and Kairiukstis, 1990).

Growth curves were then used to determine the initiation of abrupt growth reduction or recovery in the trees hit by rockfalls. Further focus was placed on the visual analysis of callus tissue overgrowing scars. In a last step, recurrence intervals of rockfalls at the tree level were determined by dividing tree age at breast height by the number of dated GD per tree.

Reconstructing rockfall rates and analysis of triggers

In contrast to other geomorphic processes that have relatively large volumes or affected areas (such as debris flows, snow avalanches or floods), rockfalls normally consist of single falling, bouncing or rolling rocks and boulders which may only hit trees along their trajectory and within a range defined by the size of the clast (Figure 4). Rather than using absolute values, we therefore use a yearly rockfall rate expressed as number of rockfall impacts per meter width of all tree surfaces present per year:

$$RR_n = (\Sigma i_n \div ED_n)$$

where RR_n stands for the rockfall rate in year n; i_n for the number of injuries in year n and ED_n for DBH (in meters) of all trees present in year n. The yearly DBH increment of each tree was obtained by dividing its current DBH by the number of rings between the innermost ring present on the core and sample year. Within this study, increment rates in trees were considered to remain constant and we willingly disregarded juvenile growth or ageing trends. The rate is based on the fact that thick stems expose a larger target (i.e. exposed diameter, ED) to falling rocks than thin ones and so large trunks would be more likely to be subject to GD.

Return periods of rockfalls were spatially visualized with the ArcGIS 9 Geostatistical Analyst software (ESRI, 2010) using an Ordinary Kriging model and based on data from five neighboring trees in general and at least two trees in angular sections.

Results

Tree age and growth disturbances

Data on the pith age of trees at sampling height indicate that the 24 *Pinus hartwegii* trees sampled are, on average, 85·8 years old (standard deviation is 39·2 years). The oldest tree sampled has 209 increment rings at sampling height (AD 1799), the youngest tree reached sampling height in AD 1984.

Analysis of the 86 increment cores allowed identification of 206 GD attributed to rockfall activity. Table I illustrates the different signs identified in the tree-ring series and points to the predominance of abrupt growth decreases (37·9%) resulting from large wounds or apex losses. Visible injuries and the presence of associated callus tissue were used for event dating in 20·4% and 19·4%, respectively. Abrupt growth releases occurred in 33 cores (16%) and compression wood was observed in 13 samples (6·3%).

Spatial distribution and return periods of events

Reconstructed rockfall activity varied across the study site. Surfaces more frequently affected by rockfalls tend to be located at the upper limit of the study site and activity slightly declines during the 25-m passage through the study corridor.

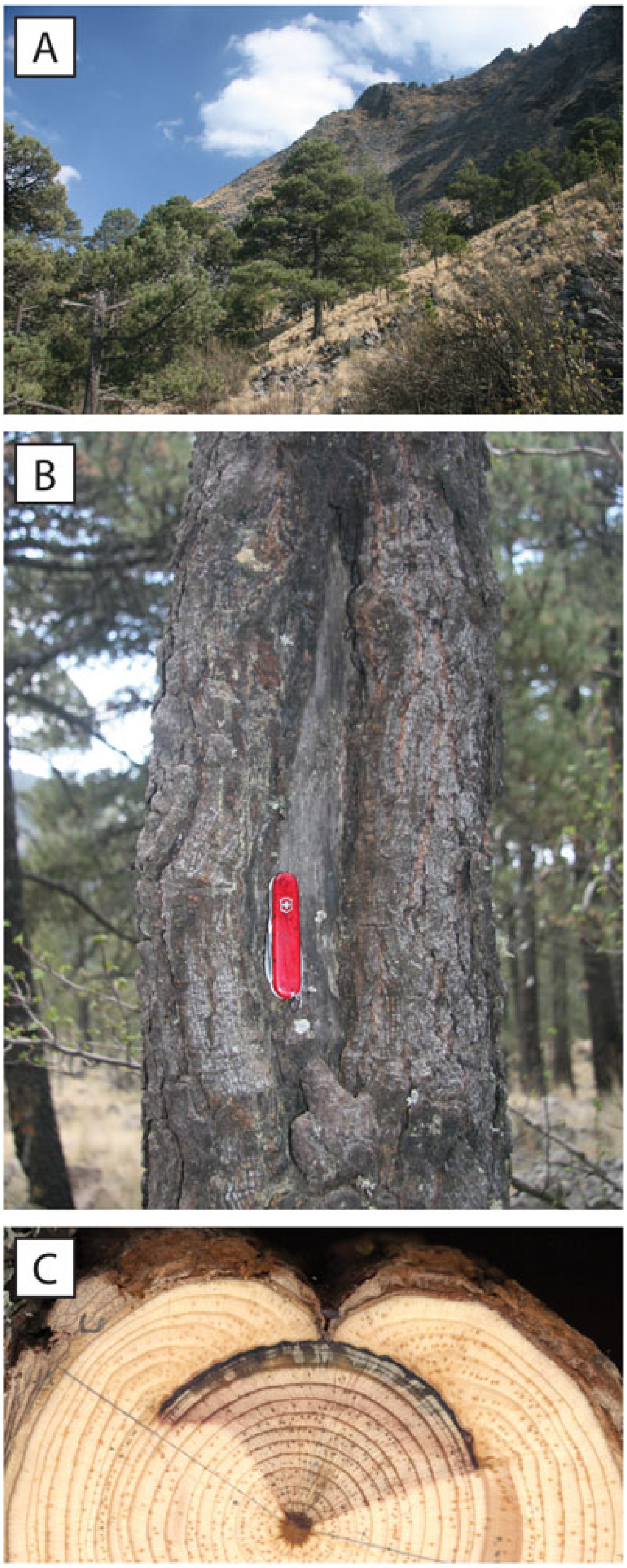

Figure 4. (A) Impression of the forest stand at Rodadero. (B) *Pinus hartwegii* tree with rockfall impact dated to 1986. (C) Detail of an overgrown injury in a juvenile *P. hartwegii* stem inflicted by rockfall activity in the year 2000. This figure is available in colour online at wileyonlinelibrary.com/journal/espl

The number of impacts and recurrence intervals at the stem level is provided in Table II, the spatial distribution of interpolated recurrence intervals is given in Figure 5. Both datasets allude to the fact that rockfall impacts recurred almost once a decade in areas with preferred rockfall trajectories and that return periods of rockfalls attain, by contrast, values of >60 years if recorder trees are protected by neighbors or other structural elements on the talus (e.g. boulders or snags).

Rockfall frequency, rockfall rate, and fluctuations in rockfall activity

Analysis of the 24 *Pinus hartwegii* samples yielded data on 67 rockfalls since AD 1836, with 94% of the reconstructed impacts dated to the past ~85 years. The remaining four rockfalls were dated to AD 1836, 1874, 1888, and 1891. These wounds were basically inflicted to the oldest tree available for this study in

Table I. Growth disturbances in *Pinus hartwegii* Lindl. trees after rockfall impacts

Growth disturbance	Absolute numbers	Relative numbers (%)
Injuries	42	20·4
Callus tissue	40	19·4
Growth decrease	78	37·9
Growth increase	33	16·0
Compression wood	13	6·3
Total	206	100

Table II. Estimation of return periods of rockfalls, depending on the availability of growth disturbances in trees

Tree	First ring	Age (years)	Tree diameter	Impacts	Return period (years)
IZT01	1899	109	35·0	3	36·3
IZT02	<1940	>68	23·6	1	68·0
IZT03	1887	121	54·1	5	24·2
IZT04	1978	30	12·7	1	30·0
IZT05	1958	50	23·9	1	50·0
IZT06	1882	126	47·7	2	63·0
IZT07	1942	66	35·0	5	13·2
IZT08	1928	80	31·8	3	26·7
IZT09	1924	84	28·6	1	84·0
IZT10	<1895	>113	35·0	3	37·7
IZT11	1955	53	30·2	4	13·3
IZT12	<1914	>94	47·7	2	47·0
IZT13	1934	74	28·6	4	18·5
IZT14	1925	83	28·6	2	41·5
IZT15	<1862	>146	28·6	5	29·2
IZT16	1915	93	50·9	4	23·3
IZT17	1945	63	9·5	3	21·0
IZT18	1940	68	20·7	1	68·0
IZT19	1932	76	27·1	2	38·0
IZT20	1984	24	9·5	1	24·0
IZT21	1938	70	25·5	2	35·0
IZT22	1948	60	22·3	2	30·0
IZT23	1909	99	35·0	5	19·8
IZT24	1799	209	44·6	5	41·8
Total	—	—	—	67	—
Mean	—	85·79	30·7	3	36·8

Note: Return periods were obtained by dividing tree age (years) by the number of reconstructed impacts. Tree diameter was derived from tree circumference measurements (resolution: 10 cm) taken at breast height.

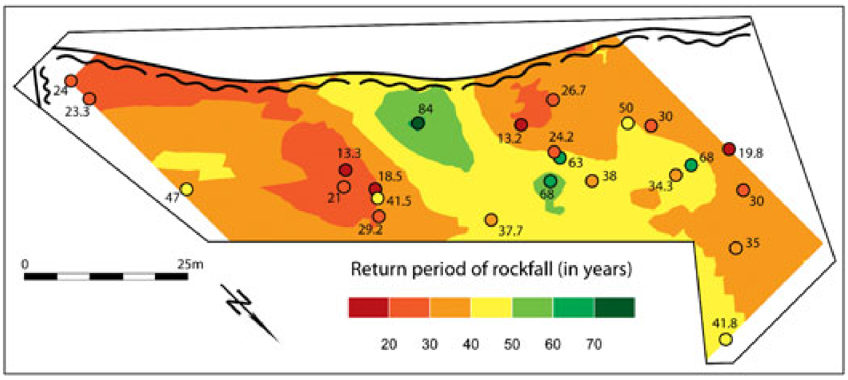

Figure 5. Interpolated return periods of rockfall impacts at the level of individual trees (in years).This figure is available in colour online at wileyonlinelibrary.com/journal/espl

the north-northwest (NNW) corner of the study site (IZT24) and at a time when the other trees did not exist. The reconstruction of rockfall frequency was therefore limited to the period 1924–2008 when at least 10 of the trees sampled on the site were available for analysis.

Based on the data obtained for individual trees, 'raw' annual rockfall frequencies were calculated; indicating the number of impacts recorded per year. As the number of trees available for analysis (i.e. sample depth in Figure 6A) increases towards the recent part of the record, there are more trees available to

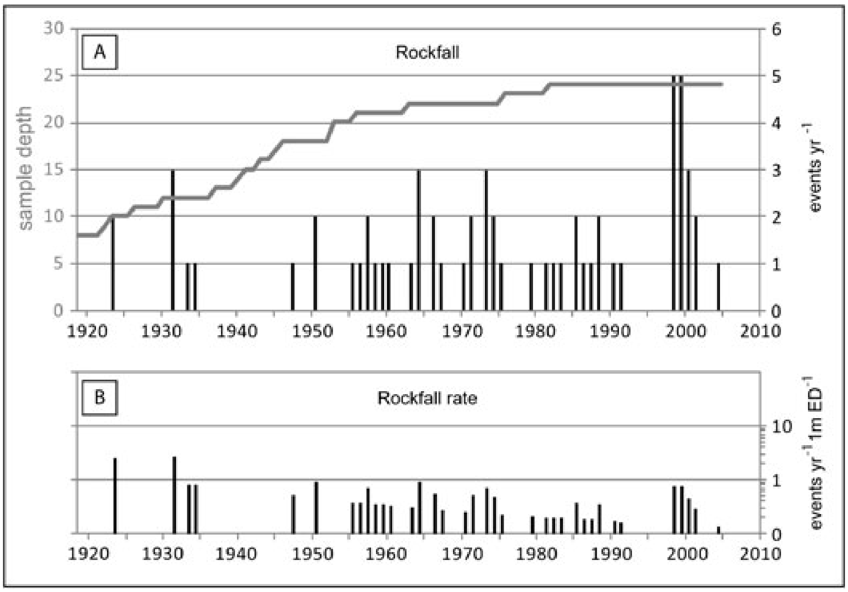

Figure 6. Minimum rockfall activity at Rodadero (Iztaccíhuatl volcano) since AD 1920: (A) If rockfall is presented as number of impacts per year, the linearly decreasing number of trees available for analysis (i.e. sample depth) will underestimate the magnitude of older and overestimate the importance of more recent events. (B) The rockfall rate takes into account the sample depth and gradual diameter increase in trees and is expressed as number of impacts per year and per 1 m exposed tree diameter (ED). For details see text and Table II.

record impacts. As a consequence, strongest rockfall activity in our data occurs in the late 1990s and the early 2000s, where a series of years with two, three, and five impacts suggests very frequent releases of rocks and boulders from the cliffs at Rodadero.

To take account of (i) changes in the number of trees available for analysis, (ii) the fact that thick stems expose a larger target (DBH) to falling rocks than thin ones, and (iii) the fact that large trunks are more likely subjected to GD, we present past rockfall activity as a 'rockfall rate'. This rate is presented in Figure 6B and expressed as number of rockfall impacts per 1 m width of all stem surfaces present per year (i.e. ED). In the early stages of the reconstruction, two and three injuries are recorded in AD 1924 and 1932, respectively, in comparably young and thin *Pinus hartwegii* stems (total ED = 0·80 and 1·13 m, respectively, in 1924 and 1932; as compared to 7·34 m in 2008). A concentration of rockfall impacts on trees also occurs between AD 1999 and 2003, but the larger overall tree surface exposed (ED) and the resulting rockfall rate presented in Figure 6B purport a less drastic increase in activity around AD 2000 than illustrated in the injury frequency plot of Figure 6A.

Irrespective of weighting, we observe distinct inter-annual variations in rockfall activity at Rodadero over the past *c.* 85 years. In particular, we observe a clustering of years with impacts in the mid-1950s to early-1960s and at the turn of the last century. In contrast, scars were not identified in the tree-rings series between 1992 and 1998 and it appears as if rockfall activity would have been less important during much of the 1980s and 1990s as compared to the time preceding and succeeding this ~20-year window. As a result of reduced sample availability and smaller EDs, injuries are also much less frequently observed in the tree-ring record for the period AD 1920–1960.

Discussion and Conclusions

In this study, the potential of dendrogeomorphic techniques has been demonstrated for a high-elevation site and in a lower-latitude geographic region where the assessment of natural hazards has often been hampered by rather limited datasets on process activity. We were successful in showing that tree-ring records of Mexican mountain pines (*Pinus hartwegii* Lindl.) can indeed be used for the analyses of geomorphic processes and that they considerably help to improve time series of rockfall events. This is promising for future research, as an overwhelming concentration of mass-wasting damage and casualties has been reported for mountain foot settlements in general and for communities in developing countries in particular (Hewitt, 1976).

Based on increment cores and cross-sections of 24 *Pinus hartwegii* trees from the foot of the Rodadero talus located on the NNE-facing slopes of Iztaccíhuatl volcano, we present a dendrogeomorphic case study and illustrate how sample depth and tree diameter (DBH) influence reconstructed rockfall rates. Analysis yielded information on 67 rockfall impacts for the period AD 1836–2008.

The reactions to rockfalls observed in the tree-ring series of *Pinus hartwegii* included mainly injuries and adjacent callus tissue. At the same time, we observe a large presence of abrupt growth decreases in the samples. Such a widespread occurrence of sudden growth decreases has been reported in other studies of *Pinus* sp. in general (Stoffel *et al.*, 2008; Bollschweiler *et al.*, 2010) and *Pinus hartwegii* in particular (Biondi, 2001; Biondi *et al.*, 2003) and probably stems from the fact that this species tends to be sensitive to water and temperature stress. The sensitivity of *Pinus* sp. to climatic parameters may therefore put certain limitations to dendrogeomorphic assessments of geomorphic process activity. In our case, signal was separated from noise by neglecting abrupt growth changes present in most samples (i.e. climate-driven) and by focusing exclusively on those changes in growth occurring in only one or a very limited number of trees in a specific year.

In addition, event dating was somehow impeded by the absence of tangential rows of traumatic resin ducts in *Pinus* sp. – a geomorphic signature in tree rings that has proved very reliable for mass-wasting studies with *Abies*, *Larix*, *Picea* or *Pseudotsuga* (e.g. Bollschweiler *et al.*, 2008; Stoffel and Hitz, 2008; Schneuwly *et al.*, 2009a; Schneuwly *et al.*, 2009b; Butler *et al.*, 2010). Dating of past events based on reaction wood is sometimes less reliable and has to be performed with caution as well, because *Pinus* sp. is known to produce this feature also for reasons other than geomorphic (i.e. heliotropism; Berthier and Stokes, 2005). In spite of these limitations, we clearly demonstrated that *P. hartwegii* has potential for dendrogeomorphic research in general and for the assessment of rockfall activity in particular.

These restrictions also give rise to the question of (i) how much of the 'real' activity can be captured in the tree-ring series; and (ii) how many trees would be needed per surface unit to obtain as complete as possible records on past rockfalls. Conifer trees are known for overgrowing wounds within a few years after an incident (Stoffel and Perret, 2006). As a consequence, increasingly larger inchoateness will occur the farther the reconstruction is extended back in time if reconstructions are limited to visible scars and the presence of abrupt changes in growth. In this study, we have accounted for this problem by limiting our reconstruction to the last *c.* 85 years, but we cannot guarantee for a complete record for this relatively recent period of the past. In addition, in contrast to areal hillslope processes where large surfaces are usually affected by events (such as floods, debris flows, landslides or snow avalanches; Stoffel *et al.*, 2010) and a multitude of trees are thus available with signs of disturbance, rockfalls normally consists of single rocks and boulders which may only hit trees along their trajectory and within a range defined by the size of the clast (Stoffel *et al.*, 2005b).

Under ideal conditions (i.e. adequate size distribution of tree diameters, high tree density, presence of shrubs, species composition), a forest can constitute an effective protection shield against rockfalls and drastically reduce the number of rocks and boulders reaching the bottom of talus slopes. Besides stopping rocks and boulders, such a forest will also register the occurrence of rockfalls beyond the foot of the talus slope and into the forest and therefore potentially rendering tree-ring based reconstructions of rockfall activity more complete. However, based on the rather limited sample analyzed in this study and the loose forest stand present at Rodadero, we realize that the ED of all trees chosen for analysis does not cover more than 7% (2008) of this imaginary shield and that values quickly drop as soon as we go back in time. In addition, we also need to be aware that trees are only surviving in sectors less exposed to rockfall activity and that woody vegetation will be largely absent in areas suffering most frequently from the passage of rocks and boulders. Based on the morphology and composition of the talus slope as well as on the deposits beyond the talus foot, small rockfalls are most likely stopped in the upper part of the non-vegetated talus slope. The large boulders (~5 m^3) present at Rodadero were transported before the current forest established and are thought to have had sufficient energy to destroy (most) vegetation along their trajectory (Dorren *et al.*, 2007). Realistic assessments of rockfall activity on forested slopes are thus difficult to achieve, unless they are based on extensive and dense sampling networks and on large sample depths (Stoffel *et al.*, 2005b; Schneuwly and Stoffel, 2008a, 2008b; Moya *et al.*, 2010). In addition, tree-ring studies should be based on 'rockfall rates' as they take account of changing 'shield' and target sizes. As shown in Figures 5A and 5B, an assessment of past rockfall activity based on injury counts alone will largely overestimate the significance of more recent events and ignore that the likelihood of rockfall impacts on trees was smaller during the first half of the twentieth century, when increment-ring records are limited to a much smaller number of predominantly young and thin trees. On the one hand, we are also aware that outweighing sample depth limitations and using ED may overlevel the events of the late 1990s and early 2000s and give, on the other hand, too much importance to the events in the 1920s and early 1930s.

In spite of these limitations, tree-ring studies have the potential to provide extensive datasets on past activity and may have advantages over other types of retrospective assessments of process activity. While short-term observations of present-day rockfall activity in the field (e.g. Luckman, 1976; Krautblatter and Dikau, 2007; Krautblatter and Moser, 2009) yields exhaustive information on current process activity on a slope, they normally fail to estimate long-term accumulation rates. Such long-term estimates of sedimentation can be derived from accumulated talus volume (Rapp, 1960) or lichenometry (André, 1997), but rates may neither be representative of contemporary rockfalls activities nor of those that prevailed in the past (Luckman and Fiske, 1995).

In this respect, dendrogeomorphology represent a suitable compromise as it yields both highly-resolved (i.e. up to seasonal dating accuracy) and long-term (i.e. several centuries) data on past rockfall activity on forested slopes, hazards and risks, especially if they combined with numerical, physically-based rockfall modeling approaches (e.g. Crosta and Agliardi, 2003; Dorren *et al.*, 2004; Stoffel *et al.*, 2006). Although the present study clearly alludes to the potential of tree-ring records for the documentation of past mass movements in low-latitude, high-altitude settings, much more data on past earth-surface processes is needed to realistically determine the role of hydrometeorological events [e.g. El Niño Southern Oscillation (ENSO) driven precipitation events] on the frequency and eventually also on the magnitude of mass-movement processes in these environments.

Acknowledgments—The authors are grateful to the referees and the managing editor S. N. Lane for insightful comments and suggestions on the manuscript. This project was funded by the Research Fund of the University of Fribourg (Grant No. 293). Nathalie Chanez is warmly acknowledged for her help during laboratory analysis and Igor Lièvre for the drafting of illustrations.

References

Alestalo J. 1971. Dendrochronological interpretation of geomorphic processes. *Fennia* **105**: 1–139.

André MF. 1997. Holocene rockwall retreat in Svalbard: a triple-rate evolution. *Earth Surface Processes and Landforms* **22**: 423–440.

Beaman JH. 1962. The timberlines of Iztaccíhuatl and Popocatépetl, Mexico. *Ecology* **43**: 377–384.

Becker A, Davenport CA. 2003. Rockfalls triggered by the A.D. 1356 Basle Earthquake. *Terra Nova* **15**: 258–264.

Berthier S, Stokes A. 2005. Phototropic response induced by wind loading in Maritime pine seedlings (*Pinus pinaster* Aït.). *Journal of Experimental Botany* **56**: 851–856.

Biondi F. 2001. A 400-year tree-ring chronology from the tropical treeline of North America. *Ambio* **30**: 162–166.

Biondi F, Estrada IG, Gavilanes Ruiz JC, Torres AE. 2003. Tree growth response to the 1913 eruption of Volcán de Fuego de Colima, Mexico. *Quaternary Research* **59**: 293–299.

Bollschweiler M, Stoffel M, Schneuwly DM, Bourqui K. 2008. Traumatic resin ducts in *Larix decidua* stems impacted by debris flows. *Tree Physiology* **28**: 255–263.

Bollschweiler M, Stoffel M, Vázquez-Selem L, Palacios D. 2010. Tree-ring reconstruction of past lahar activity at Popocatépetl volcano, Mexico. *The Holocene* **20**: 265–274.

Bräker OU. 2002. Measuring and data processing in tree-ring research – a methodological introduction. *Dendrochronologia* **20**: 203–216.

Butler DR, Sawyer CF, Maas JA. 2010. Tree-ring dating of snow avalanches in Glacier National Park, Montana, USA. In *Tree rings and natural hazards – A state-of-the-art*, Stoffel M, Bollschweiler M, Butler DR, Luckman BH (eds). Springer: Berlin, Heidelberg, New York.

Cardinali M, *et al.*, 2006. Rainfall induced landslides in December 2004 in south-western Umbria, central Italy: types, extent, damage and risk assessment. *Natural Hazards and Earth System Sciences* **6**: 237–260.

Cook ER, Kairiukstis LA. 1990. *Methods of dendrochronology – Applications in the environmental sciences*. Kluwer: London.

Crosta GB, Agliardi F. 2003. A methodology for physically based rockfall hazard assessment. *Natural Hazards and Earth System Sciences* **3**: 407–422.

Dorren LKA. 2003. A review of rockfall mechanics and modelling approaches. *Progress in Physical Geography* **27**: 69–87.

Dorren LKA, Berger F, Jonnson M, Krautblatter M, Moelk M, Stoffel M., Wehrli A. 2007. State of the art in rockfall – forest interactions. *Schweizerische Zeitschrift für Forstwesen* **158**: 128–141.

Dorren LKA, Maier B, Putters US, Seijmonsbergen AC. 2004. Combining field and modelling techniques to assess rockfall dynamics on a protection forest hillslope in the European Alps. *Geomorphology* **57**: 151–167.

ESRI. 2010. Geostatistical Analyst. www.esri.com/software/arcgis/arcgisextensions/geostatistical/ [accessed on 8 December 2010].

Gruber S, Hoelzle M, Haeberli W. 2004. Permafrost thaw and destabilization of Alpine rock walls in the hot summer of 2003. *Geophysical Research Letters* **31**: L13504.

Guzzetti F, Reichenbach P. 2010. Rockfalls and their hazards. In *Tree rings and natural hazards – A state-of-the-art*, Stoffel M, Bollschweiler M, Butler DR, Luckman BH (eds). Springer: Berlin, Heidelberg, New York.

Harp EL, Wilson RC. 1995. Shaking intensity thresholds for rock falls and slides: Evidence from 1987 Whittier Narrows and superstition hills earthquake strong-motion records. *Bulletin of the Seismological Society of America* **85**: 1739–1757.

Hewitt K. 1976. Earthquake hazards in the mountains. *Natural History* **85**: 30–37.

Krautblatter M, Dikau R. 2007. Towards a uniform concept for the comparison and extrapolation of rockwall retreat and rockfall supply. *Geografiska Annaler* **89A**: 21–40.

Krautblatter M, Moser M. 2009. A nonlinear model coupling rockfall and rainfall intensity based on a four year measurement in a high Alpine rock wall (Reintal, German Alps). *Natural Hazards and Earth System Sciences* **9**: 1425–1432.

Lauer W. 1978. Timberline studies in Central Mexico. *Arctic and Alpine Research* **10**: 383–396.

Luckman BH. 1976. Rockfalls and rockfall inventory data – some observations from Surprise Valley, Jasper National Park, Canada. *Earth Surface Processes* **1**: 287–298.

Luckman BH. 2007. Talus slopes. In *Encyclopedia of Quaternary Science*, Elias SA (ed.). Elsevier: Oxford; 2242–2249.

Luckman BH, Fiske CJ. 1995. Estimating long-term rockfall accretion rates by lichenometry. In *Steepland Geomorphology*, Slaymaker O (ed.). Wiley: Chichester; 233–255.

Marzorati S, Luzi L, De Amicis M. 2002. Rock falls induced by earthquakes: a statistical approach. *Soil Dynamics and Earthquake Engineering* **22**: 565–577.

Matsuoka N, Murton J. 2008. Frost weathering: Recent advances and future directions. *Permafrost and Periglacial Processes* **19**: 195–210.

Matsuoka N, Sakai H. 1999. Rockfall activity from an alpine cliff during thawing periods. *Geomorphology* **28**: 309–328.

Moya J, Corominas J, Pérez Arcas J. 2010. Assessment of the rockfall frequency for hazard analysis at Solà d'Andorra (eastern Pyrenees). In *Tree Rings and Natural Hazards – A State-of-the-art*, Stoffel M, Bollschweiler M, Butler, DR, Luckman BH (eds). Springer: Berlin.

Nixon GT. 1989. The Geology of Iztaccíhuatl volcano and adjacent areas of the Sierra Nevada and Valley of Mexico. *Geological Society of America Special Paper* **129**: 1–58.

Perret S, Stoffel M, Kienholz H. 2006. Spatial and temporal rockfall activity in a forest stand in the Swiss Prealps – a dendrogeomorphological case study. *Geomorphology* **74**: 219–231.

Rapp A. 1960. Recent development of mountain slopes in Kärkevagge and surroundings, northern Scandinavia. *Geografiska Annaler* **42**: 65–200.

Rinntech. 2010. *LINTAB – Precision Ring by Ring*, http://www.rinntech.com/Products/Lintab.htm [accessed on 8 December 2010].

Schneuwly DM, Stoffel M. 2008a. Spatial analysis of rockfall activity, bounce heights and geomorphic changes over the last 50 years – a case study using dendrogeomorphology. *Geomorphology* **102**: 522–531.

Schneuwly DM, Stoffel M. 2008b. Tree-ring based reconstruction of the seasonal timing, major events and origin of rockfall on a case-study slope in the Swiss Alps. *Natural Hazards and Earth System Sciences* **8**: 203–211.

Schneuwly DM, Stoffel M, Bollschweiler M. 2009a. Formation and spread of callus tissue and tangential rows of resin ducts in *Larix decidua* and *Picea abies* following rockfall impacts. *Tree Physiology* **29**: 281–289.

Schneuwly DM, Stoffel M, Dorren LKA, Berger F. 2009b. Three-dimensional analysis of the anatomical growth response of European conifers to mechanical disturbance. *Tree Physiology* **29**: 1247–1257.

Shroder JF. 1978. Dendrogeomorphological analysis of mass movement on Table Cliffs Plateau, Utah. *Quaternary Research* **9**: 168–185.

Siebe C, Abrams M, Luis Macías J, Obenholzner J. 1996. Repeated volcanic disasters in Prehispanic time at Popocatépetl, central Mexico: past key to the future? *Geology* **24**: 399–402.

Stoffel M. 2005. Assessing the vertical distribution and visibility of scars in trees. *Schweizerische Zeitschrift für das Forstwesen* **156**: 195–199.

Stoffel M. 2006. A review of studies dealing with tree rings and rockfall activity: the role of dendrogeomorphology in natural hazard research. *Natural Hazards* **39**: 51–70.

Stoffel M, Bollschweiler M. 2008. Tree-ring analysis in natural hazards research – an overview. *Natural Hazards and Earth System Sciences* **8**: 187–202.

Stoffel M, Bollschweiler M, Butler DR, Luckman BH. 2010. *Tree Rings and Natural Hazards – A State-of-the-art*. Springer: Heidelberg.

Stoffel M, Bollschweiler M, Leutwiler A, Aeby P. 2008. Tree-ring reconstruction of debris-flow events leading to overbank sedimentation on the Illgraben cone (Valais Alps, Switzerland). *The Open Geology Journal* **2**: 18–29.

Stoffel M, Hitz OM. 2008. Rockfall and snow avalanche impacts leave different anatomical signatures in tree rings of juvenile *Larix decidua*. *Tree Physiology* **28**: 1713–1720.

Stoffel M, Lièvre I, Monbaron M, Perret S. 2005a. Seasonal timing of rockfall activity on a forested slope at Täschgufer (Swiss Alps) – a dendrochronological approach. *Zeitschrift für Geomorphologie* **49**: 89–106.

Stoffel M, Perret S. 2006. Reconstructing past rockfall activity with tree rings: some methodological considerations. *Dendrochronologia* **24**: 1–15.

Stoffel M, Schneuwly D, Bollschweiler M, Lièvre I, Delaloye R, Myint M., Monbaron M. 2005b. Analyzing rockfall activity (1600–2002) in a protection forest – a case study using dendrogeomorphology. *Geomorphology* **68**: 224–241.

Stoffel M, Wehrli A, Kühne R, Dorren LKA, Perret S, Kienholz H. 2006. Assessing the protective effect of mountain forests against rockfall using a 3D simulation model. *Forest Ecology and Management* **225**: 113–122.

Vázquez-Selem L. 1997. Late Quaternary glaciations of Téyotl volcano, central Mexico. *Quaternary International* **43**: 67–73.

Vázquez-Selem L, Heine K. 2004. Late Quaternary glaciation of Mexico. In *Quaternary Glaciations – Extent and Chronology. Part III: South America, Asia, Africa, Australia, Antarctica*, Ehlers J, Gibbard PL (eds). Elsevier: Amsterdam; 233–242.

White SE. 1962. Late Pleistocene glacial sequence for the west side of Iztaccíhuatl Volcano, México. *Geological Society of America Bulletin* **73**: 935–958.

